J. Fluid Mech. (2011), *vol.* 668, *pp.* 335–350. © Cambridge University Press 2010
doi:10.1017/S0022112010004672

Flow decomposition and aerodynamic sound generation

SAMUEL SINAYOKO[1], A. AGARWAL[1]† AND Z. HU[2]

[1]Institute of Sound and Vibration Research, University of Southampton, Southampton S017 1BJ, UK

[2]School of Engineering Sciences, University of Southampton, Southampton S017 1BJ, UK

(Received 23 December 2009; revised 7 September 2010; accepted 8 September 2010; first published online 3 December 2010)

An approximate decomposition of fluid-flow variables satisfying unbounded compressible Navier–Stokes equations into acoustically radiating and non-radiating components leads to well-defined source terms that can be identified as the physical sources of aerodynamic noise. We show that, by filtering the flow field by means of a linear convolution filter, it is possible to decompose the flow into non-radiating and radiating components. This is demonstrated on two different flows: one satisfying the linearised Euler equations and the other the Navier–Stokes equations. In the latter case, the corresponding sound sources are computed. They are found to be more physical than those computed through classical acoustic analogies in which the flow field is decomposed into a steady mean and fluctuating component.

Key words: aeroacoustics, jet noise

1. Introduction

Despite more than 50 years of research in aeroacoustics, controlling the sound radiated by turbulent jets remains difficult. One reason is that no definite answer has been found on how turbulent flows generate sound. A major obstacle is the lack of understanding of the physical sources of sound in a jet.

One way to derive the aerodynamic noise sources is to use an acoustic analogy. In general this involves rearranging the Navier–Stokes equations to have a wave-propagation operator that is linear about a steady base flow on the left-hand side; the remaining terms are grouped as sources on the right-hand side. The underlying assumption is the absence of feedback between the hydrodynamic field and the acoustic field. Goldstein (2003) provides a good generalisation of such approaches. The fluctuating variables on the left-hand side are the dependent variables of the problem and represent both acoustic and hydrodynamic waves. This implies that the sources on the right-hand side cannot be identified as just sound sources. Furthermore, we expect the sound field to be a small by-product of the hydrodynamic field. The sound source should be a function of the hydrodynamic field only. This property is not satisfied by traditional acoustic analogies.

An alternative method for identifying the physical sound sources was proposed by Goldstein (2005). He suggested that if an unbounded turbulent field could be

† Present address: Department of Engineering, University of Cambridge, Trumpington Street, Cambridge CB2 1PZ. Email address for correspondence: aa406@cam.ac.uk

separated into acoustically radiating and non-radiating components, then the resulting sources should approach the true sources of aerodynamically generated sound. The present paper is inspired by Goldstein's work.

We show that it is indeed possible to separate radiating acoustic components from non-radiating components in nonlinear fluid-flow equations by using linear convolution filters. We also show that, following such a decomposition, the sound sources depend only on the non-radiating field. The source terms do not contain the dependent radiating variables and should therefore represent the true sources of sound. We present a simple expression for the source terms. It is almost identical to the one derived by Goldstein. However, our result is approximate because we assume homentropy and ignore terms which are quadratic in the radiating variables. These choices simplify the derivation of the sources and should have little consequence for the flows we are studying here. The source expression we derive is therefore approximate, but an exact set of equations for the general case can be found in Goldstein (2005). In addition, we show that Goldstein's sound sources can be further decomposed to identify the pure acoustic sources.

This paper is organised as follows. In § 2, we present an expression for aerodynamic noise sources. In § 3, we show how to construct a non-radiating filter for a simple example of harmonically excited parallel flow satisfying the linearised Euler equations. Then, in § 4, we apply a similar filtering procedure to an axisymmetric jet, excited at the inflow by two frequencies, that satisfies an inhomogeneous version of the Navier–Stokes equations. The non-radiating base flow is used to compute the corresponding sound sources.

2. Aerodynamic noise sources

2.1. *Flow decomposition*

For an unbounded flow field surrounded by a quiescent ambient medium, the radiating components are those which satisfy the dispersion relation $|\boldsymbol{k}| = |\omega|/c_\infty$ (Crighton 1975; Dowling & Ffowcs Williams 1983; Goldstein 2005), where $\boldsymbol{k}$ denotes the wavenumber, ω is the angular frequency and c_∞ is the ambient speed of sound. The non-radiating components are those which do not satisfy the above dispersion relation.

As pointed out by Goldstein (2005), it is difficult to identify the acoustic components within the unsteady flow region. In this paper, for definiteness, we identify the acoustic components with the radiating part of the flow field, which we have defined in the preceding paragraph. The hydrodynamic field is considered to be the unsteady part of the non-radiating field.

Let $\mathscr{L}$ be a linear filter that captures the entire non-radiating part of a flow variable. Any flow variable q can then be decomposed as

$$q = \overline{q} + q', \tag{2.1}$$

where $\overline{q} \equiv \mathscr{L}q$ represents the non-radiating part of q and q' contains only the radiating components. The radiating components can also be obtained directly by applying the linear filter $\mathscr{L}'$ defined as

$$\mathscr{L}' \equiv \mathscr{I} - \mathscr{L}, \tag{2.2}$$

where $\mathscr{I}$ denotes the identity operator.

2.2. *Source definition*

The flow variables satisfy the Navier–Stokes equations as

$$\frac{\partial \rho}{\partial t} + \frac{\partial}{\partial x_j}\rho v_j = 0, \tag{2.3}$$

$$\frac{\partial}{\partial t}\rho v_i + \frac{\partial}{\partial x_j}\rho v_i v_j + \frac{\partial p}{\partial x_i} = \frac{\partial}{\partial x_j}\sigma_{ij}, \tag{2.4}$$

where ρ, p and $\boldsymbol{v} = (v_i)$ denote the density, pressure and flow velocity and σ_{ij} is the viscous stress tensor. We assume that the flow is homentropic, so $\sigma_{ij} = 0$. For a perfect gas, we have the energy equation as (Goldstein 1976)

$$\frac{\partial p}{\partial t} + v_j \frac{\partial p}{\partial x_j} + \gamma p \frac{\partial v_j}{\partial x_j} = 0. \tag{2.5}$$

Introducing the variable $\pi \equiv p^{1/\gamma}$ allows us to rewrite (2.4) and (2.5) in conservative form as (Lilley 1974)

$$\frac{\partial}{\partial t}\rho v_i + \frac{\partial}{\partial x_j}\rho v_i v_j + \frac{\partial}{\partial x_i}\pi^\gamma = 0, \tag{2.6}$$

$$\frac{\partial \pi}{\partial t} + \frac{\partial}{\partial x_j}\pi v_j = 0. \tag{2.7}$$

Applying $\mathscr{L}'$ to (2.3), (2.6) and (2.7) gives the governing equations for the radiating components:

$$\frac{\partial \rho'}{\partial t} + \frac{\partial}{\partial x_j}(\rho v_j)' = 0, \tag{2.8}$$

$$\frac{\partial}{\partial t}(\rho v_i)' + \frac{\partial}{\partial x_j}(\rho v_i v_j)' + \frac{\partial}{\partial x_i}(\pi^\gamma)' = 0, \tag{2.9}$$

$$\frac{\partial \pi'}{\partial t} + \frac{\partial}{\partial x_j}(\pi v_j)' = 0. \tag{2.10}$$

We rewrite each of the above equations to obtain an operator that is linear in the radiating dependent variables $\{\rho'$, $(\rho v_i)'$ and $\pi'\}$ on the left-hand side. In (2.9), the term $\rho v_i v_j$ can be expanded by decomposing each of the flow variables using (2.1)

$$\begin{aligned}\rho v_i v_j = \frac{\rho v_i \rho v_j}{\rho} &= \frac{\overline{\rho v_i}\,\overline{\rho v_j}}{\overline{\rho}} + \frac{\overline{\rho v_j}}{\overline{\rho}}(\rho v_i)' + \frac{\overline{\rho v_i}}{\overline{\rho}}(\rho v_j)' - \frac{\overline{\rho v_i}\,\overline{\rho v_j}}{\overline{\rho}^2}\rho' + O(\rho'^2),\\ &= \overline{\rho}\,\widetilde{v}_i\widetilde{v}_j + \widetilde{v}_j(\rho v_i)' + \widetilde{v}_i(\rho v_j)' - \widetilde{v}_i\widetilde{v}_j\rho' + O(\rho'^2),\end{aligned} \tag{2.11}$$

where we have introduced

$$\widetilde{v}_i = \frac{\overline{\rho v_i}}{\overline{\rho}}, \tag{2.12}$$

so that $\widetilde{v}_i$ represents Favre-averaged v_i, and where $O(\rho'^2)$ represents terms that are at least quadratic in the radiating variables. Because the radiating part of the flow is normally several orders of magnitude smaller than the non-radiating part, these higher-order terms are expected to be small and will be neglected. Applying $\mathscr{L}'$ to (2.11) gives

$$(\rho v_i v_j)' \approx \underbrace{(\overline{\rho}\,\widetilde{v}_i\widetilde{v}_j)'}_{(b)} + \underbrace{(\widetilde{v}_j(\rho v_i)' + \widetilde{v}_i(\rho v_j)' - \widetilde{v}_i\widetilde{v}_j\rho')'}_{(a)}. \tag{2.13}$$

We assume a one-way coupling between hydrodynamics and acoustics: the hydrodynamic field is responsible for the production of sound, but the sound field does not affect the hydrodynamic field. Therefore, the source of sound must be independent of the radiating components. The only terms satisfying this requirement are those in group (b) of (2.13). The terms in group (a) of (2.13) involve a radiating component interacting with the non-radiating base flow. These terms represent propagation effects such as refraction and can be excluded from the source. The other nonlinear term in (2.9) is $(\pi^\gamma)'$ which can be decomposed as follows:

$$\pi^\gamma = (\overline{\pi} + \pi')^\gamma = \overline{\pi}^\gamma + \gamma \overline{\pi}^{\gamma-1}\pi' + O(\pi'^2), \tag{2.14}$$

$$(\pi^\gamma)' \approx \underbrace{(\overline{\pi}^\gamma)'}_{(b)} + \underbrace{(\gamma \overline{\pi}^{\gamma-1}\pi')'}_{(a)}. \tag{2.15}$$

However, π^γ can also be expressed as

$$\pi^\gamma = p = \overline{p} + p', \tag{2.16}$$

so, by identifying the zeroth and first-order terms between (2.14) and (2.16),

$$\overline{p} = \overline{\pi}^\gamma, \quad p' \approx \gamma \overline{\pi}^{\gamma-1}\pi'. \tag{2.17}$$

From (2.17) we can write $(\overline{\pi}^\gamma)' = (\overline{p})' = 0$, so the source term ($b$) of (2.15) is equal to zero.

Similarly, in (2.10), $(\pi v_j)'$ can be decomposed as follows:

$$(\pi v_j)' \approx \underbrace{(\overline{\pi}\widetilde{v_j})'}_{(b)} + \underbrace{\left(\frac{\overline{\pi}}{\overline{\rho}}(\rho v_j)' + \widetilde{v_j}\pi' - \frac{\overline{\pi}}{\overline{\rho}}\widetilde{v_j}\rho'\right)'}_{(a)}. \tag{2.18}$$

Since the flow is assumed to be homentropic,

$$p = \alpha\rho^\gamma, \quad \overline{p} = \alpha\overline{\rho}^\gamma, \quad p' = \alpha\gamma\overline{\rho}^{\gamma-1}\rho', \tag{2.19}$$

where α is a constant. From (2.17), (2.19) and (2.12), it can be seen that

$$(\overline{\pi}\widetilde{v_j})' = \alpha^{1/\gamma}(\overline{\rho}\widetilde{v_j})' = \alpha^{1/\gamma}(\overline{\rho v_j})' = 0, \tag{2.20}$$

so the source term (b) in (2.18) is equal to zero.

We can now rewrite equations (2.8)–(2.10) by pushing the sound source (b) of (2.13) to the right-hand side, and leaving the interaction terms (a) on the left-hand side, which gives

$$\frac{\partial\rho'}{\partial t} + \frac{\partial}{\partial x_j}(\rho v_j)' = 0, \tag{2.21}$$

$$\frac{\partial}{\partial t}(\rho v_i)' + \frac{\partial}{\partial x_j}\left[\widetilde{v_j}(\rho v_i)' + \widetilde{v_i}(\rho v_j)' - \widetilde{v_i}\widetilde{v_j}\rho'\right]' + \gamma\frac{\partial}{\partial x_i}\left[\overline{\pi}^{\gamma-1}\pi'\right]' = f_{1i}, \tag{2.22}$$

$$\frac{\partial\pi'}{\partial t} + \frac{\partial}{\partial x_j}\left[\frac{\overline{\pi}}{\overline{\rho}}[(\rho v_j)' - \widetilde{v_j}\rho'] + \widetilde{v_j}\pi'\right]' = 0, \tag{2.23}$$

where the momentum equation source term f_{1i} is defined as

$$f_{1i} \equiv -\frac{\partial}{\partial x_j}(\overline{\rho}\,\widetilde{v_i}\widetilde{v_j})'. \tag{2.24}$$

The equation shows that the noise source f_{1i} is a radiating quantity; this is what we expect because the left-hand side of (2.21)–(2.23) depends linearly on the radiating variables. This means that f_{1i} produces only acoustic waves. Also, as we expect, the

source is expressed as a (nonlinear) function of only the non-radiating components: it is free of the dependent (radiating) variables. Therefore, this source should represent the true source of aerodynamically generated sound. These key features distinguish the present source from past representations based on classical acoustic analogies.

Note that for a homentropic flow, no sound source is present in the energy equation (2.23). In the general case, we would expect to have additional sources. Assuming homentropy is mostly applicable to low-Mach-number flows, the above procedure could be extended by using a more general energy equation.

2.2.1. *Comparison with Goldstein's approach*

The present approach differs from that of Goldstein (2005). Our expression is valid only for homentropic flows and is only approximate because we neglect quadratic terms in radiating quantities. Secondly, we use a different set of dependent radiating variables. However, the two sources are related. If we assume homentropy and neglect quadratic terms in radiating quantities, Goldstein's sound sources (Goldstein 2009, equation (2.12)) can be expressed as

$$f_{gi} \approx \frac{\partial}{\partial x_j}(\overline{\rho v_i v_j} - \overline{\rho}\,\widetilde{v}_i\widetilde{v}_j). \tag{2.25}$$

Applying $\mathscr{L}$ to (2.11) and substituting the result into (2.25) gives

$$\begin{aligned} f_{gi} &\approx \frac{\partial}{\partial x_j}\left(\overline{\overline{\rho}\,\widetilde{v}_i\widetilde{v}_j} + \overline{\widetilde{v}_j(\rho v_i)'} + \overline{\widetilde{v}_i(\rho v_j)'} - \overline{\widetilde{v}_i\widetilde{v}_j\rho'} - \overline{\rho}\,\widetilde{v}_i\widetilde{v}_j\right) \\ &= \underbrace{-\frac{\partial}{\partial x_j}(\overline{\rho}\,\widetilde{v}_i\widetilde{v}_j)'}_{(a)} + \underbrace{\frac{\partial}{\partial x_j}\left[\overline{\widetilde{v}_j(\rho v_i)'} + \overline{\widetilde{v}_i(\rho v_j)'} - \overline{\widetilde{v}_i\widetilde{v}_j\rho'}\right]}_{(b)}. \end{aligned} \tag{2.26}$$

Terms in (b) of (2.26) are clearly non-radiating and can be taken out of the source. This leaves the source term (a) of (2.26), which is identical to f_{1i}.

2.2.2. *Physical interpretation for the propagation operator*

The terms within the square brackets on the left-hand side of (2.21)–(2.23) can be interpreted as follows. Each non-radiating term, e.g. $\widetilde{v}_i$, can be decomposed into a steady-mean part v_{i0} and an unsteady part v_{ih}, which represents hydrodynamic components. If we assume that $v_i' \ll v_{ih} \ll v_{i0}$, then the leading-order term in $\widetilde{v}_i\widetilde{v}_j\rho'$ is $v_{i0}v_{j0}\rho'$, which is a radiating term. Then we can write

$$(\widetilde{v}_i\widetilde{v}_j\rho')' = \widetilde{v}_i\widetilde{v}_j\rho' - \overline{\widetilde{v}_i\widetilde{v}_j\rho'} \approx v_{i0}v_{j0}\rho'. \tag{2.27}$$

Note that these approximations are not always accurate and are not necessary for the flow decomposition or the derivation of the true sources of sound (see Sinayoko & Agarwal 2010*a* for more details). Following such an approximation, the interactions between radiating and non-radiating components reduce to interactions between radiating components and the steady-mean flow, and (2.21)–(2.23) become inhomogeneous Euler equations linearised about a steady base flow.

2.2.3. *Wave-like equation*

We can obtain a wave-like equation by taking ∂ (2.22)$/\partial x_i - \partial$ (2.21)$/\partial t$ and expressing π' in terms of ρ' using (2.17) and (2.19), which gives

$$\frac{\partial^2}{\partial x_i \partial x_i}(\overline{c}^2\rho') - \frac{\partial^2\rho'}{\partial t^2} + \frac{\partial^2}{\partial x_i \partial x_j}(\widetilde{v}_j(\rho v_i)' + \widetilde{v}_i(\rho v_j)' - \widetilde{v}_i\widetilde{v}_j\rho')' = s_1, \tag{2.28}$$

where $\overline{c}^2 = \gamma\overline{p}/\overline{\rho}$ and the noise source s_1 is defined as

$$s_1 \equiv \frac{\partial f_{1i}}{\partial x_i} = -\frac{\partial^2}{\partial x_i \partial x_j}(\overline{\rho}\,\widetilde{v}_i\widetilde{v}_j)'. \tag{2.29}$$

Equation (2.28) reduces to a homogeneous second-order wave equation outside the jet. Using s_1 allows us to express the source of noise with a single term. Although the sources f_{1i} given by (2.24) are well defined, s_1 is used for convenience. It does not significantly alter the magnitude or structure of the sources and provides a convenient way to compare different types of sources.

2.3. *Non-radiating filters*

Applying the Fourier transform (FT) to the filtered variable $\overline{q}$ gives

$$\overline{Q}(\boldsymbol{k}, \omega) = \int_{-\infty}^{+\infty} \int_{\mathscr{V}} \overline{q}(\boldsymbol{x}, t) \mathrm{e}^{\mathrm{i}(\omega t - \boldsymbol{k}\cdot\boldsymbol{x})}\, \mathrm{d}^3\boldsymbol{x}\, \mathrm{d}t, \tag{2.30}$$

where $\mathscr{V}$ denotes the entire spatial domain. Goldstein (2005) showed that, for an unbounded turbulent flow through a quiescent medium, if

$$\overline{Q}(\boldsymbol{k}, \omega) = 0, \quad \text{when} \quad |\boldsymbol{k}| = |\omega|/c_\infty, \tag{2.31}$$

then $\overline{q}$ does not contain any radiating component. We call non-radiating filters those linear filters that satisfy (2.31).

We need a filter that captures the entire non-radiating part of the flow without distorting it. To achieve this, the filter should also satisfy the following condition:

$$\overline{Q}(\boldsymbol{k}, \omega) = Q(\boldsymbol{k}, \omega), \quad \text{when} \quad |\boldsymbol{k}| \neq |\omega|/c_\infty. \tag{2.32}$$

We call the filters that satisfy conditions (2.31) and (2.32) optimal non-radiating filters. These filters allow us to decompose a flow variable into its non-radiating and radiating parts. Such decomposition is desirable because, as shown in § 2.2, it leads to an unambiguous expression for the sound sources.

Equation (2.31) corresponds to the dispersion relation for acoustic waves in a quiescent medium. For that reason, it is sometimes considered inappropriate for the study of sound sources in a moving fluid. However, the analytical proof by Crighton (1975) and Goldstein (2005) shows that, for an unbounded fluid flow surrounded by a quiescent medium, it is sufficient to satisfy (2.31) to render the flow non-radiating. The only caveat is that the filter should take into account the presence of singularities (in the spectral domain) among radiating components, a point already stressed by Goldstein (2009): the filter should go to zero sufficiently quickly to remove radiating components.

We use two approaches to the design of non-radiating filters: one involves differential operators, which can be readily implemented in the space–time domain, while the other uses a convolution operation, implemented as a product in the wavenumber–frequency domain.

2.3.1. *Differential filter*

Obtaining an optimal non-radiating filter in the space–time domain is desirable because it could be implemented easily within explicit time-domain methods used for solving the Navier–Stokes equations. One example of a non-radiating filter in the space–time domain is the d'Alembertian operator, defined by

$$\Box^2 = \frac{1}{c_\infty^2}\frac{\partial^2}{\partial t^2} - \nabla^2. \tag{2.33}$$

If $\overline{q} = \Box^2 q$, then it can be easily shown that

$$\overline{Q}(\boldsymbol{k}, \omega) = \left(|\boldsymbol{k}|^2 - \frac{\omega^2}{c_\infty^2} \right) Q(\boldsymbol{k}, \omega). \tag{2.34}$$

If $Q(\boldsymbol{k}, \omega)$ is not singular when $|\boldsymbol{k}| = |\omega|/c_\infty$, then (2.34) proves that $\overline{Q}$ satisfies (2.31). Such singularity would occur, for example, if q was a solution of the wave equation $\Box^2 q = s$, where s is a source having radiating components. However, it would generally not be the case for the flow solutions we are studying here. The d'Alembertian filter can be used directly in the space–time domain, using (2.33), or by windowing in the wavenumber–frequency domain, using (2.34).

2.3.2. *Convolution filters*

Convolution filters are of the form

$$\overline{q}(\boldsymbol{x}, t) = w * q(\boldsymbol{x}, t) = \int_{-\infty}^{+\infty} \int_{\mathscr{V}} w(\boldsymbol{y}, \tau) q(\boldsymbol{x} - \boldsymbol{y}, t - \tau) \, \mathrm{d}^3 \boldsymbol{y} \, \mathrm{d}\tau, \tag{2.35}$$

where w is a function defining the behaviour of the filter. These filters use information from the entire signal q, which gives more flexibility to extract the desired features from q. In addition, from the convolution theorem, the Fourier transform of (2.35) is given by

$$\overline{Q}(\boldsymbol{k}, \omega) = W(\boldsymbol{k}, \omega) Q(\boldsymbol{k}, \omega). \tag{2.36}$$

Convolution filters can therefore be conveniently applied as windowing operations in the frequency domain. For signals that involve large sets of data, this is more efficient than using (2.35).

The problem is then to define an appropriate window W, in the wavenumber–frequency domain, that renders the corresponding filter w, in the space–time domain, non-radiating. For an optimal non-radiating filter, the window $W(\boldsymbol{k}, \omega)$ should be such that

$$W(\boldsymbol{k}, \omega) = 0, \quad \text{if} \quad |\boldsymbol{k}| = |\omega|/c_\infty, \tag{2.37}$$

$$W(\boldsymbol{k}, \omega) = 1, \quad \text{if} \quad |\boldsymbol{k}| \neq |\omega|/c_\infty. \tag{2.38}$$

If both equations are satisfied then the radiating part occupies zero volume in the wavenumber–frequency domain. As Goldstein (2009) notes, this property is not necessarily a problem; for example, time-average filters have zero volume in the wavenumber–frequency domain. However, in practice, for a solution of the Navier–Stokes equations, there should be some separation between the radiating components lying on the radiation circle ($|\boldsymbol{k}| = |\omega|/c_\infty$) and the non-radiating components ($|\boldsymbol{k}| \neq |\omega|/c_\infty$). Therefore, it is possible to use a filter window of finite width. This separation between radiating and non-radiating components may not materialise in transonic and supersonic flows, thus limiting the present approach to subsonic flows.

An alternative method for defining a non-radiating convolution filter is to focus on capturing the main hydrodynamic components of the flow. A prior understanding of the hydrodynamic content of the flow is required to do so. Such understanding can be obtained by a careful analysis of the Fourier transform of the flow field as will be shown in § 3.

Several investigators have used filtering techniques in the wavenumber–frequency domain to separate the radiating and non-radiating parts of the flow within the framework of Lighthill's acoustic analogy. Freund (2001) used the criterion

$|k_z| < |\omega|/c_\infty$ to extract the radiating part of Lighthill's source term in a turbulent jet, where k_z denotes the axial wavenumber, ω is the angular frequency and c_∞ is the ambient speed of sound. Cabana, Fortuné & Jordan (2008) and Tinney & Jordan (2008) applied the same criterion, respectively, to Lighthill's source term in a temporal mixing layer, and to pressure measurements in the near field of a co-axial jet. It is important to notice, as Freund (2001) did, that this criterion neglects the radial structure of the flow (wavenumber k_r in the radial direction). Therefore, in certain cases, using a filtering criterion based on only the axial wavenumber is not sufficient to separate the radiating and non-radiating components. For example, for a given k_z, even if $|k_z| < |\omega|/c_\infty$, k_r could be large enough to have $|\boldsymbol{k}| = \sqrt{k_z^2 + k_r^2}$ greater than $|\omega|/c_\infty$. A radiating filter based only on $|k_z| < |\omega|/c_\infty$ can therefore capture some of the non-radiating components. The complete criterion is given by (2.31) and (2.32).

One drawback of using convolution filters is that (2.21)–(2.23) becomes a system of integro-differential equations, which is difficult to solve. However, one does not have to solve this system to compute the sound sources. As we demonstrate in § 4, the sound sources can be computed by applying the filter to flow solutions obtained by direct numerical simulation.

3. Filtering a two-dimensional parallel shear layer flow

3.1. *Problem description and implementation*

We apply the filtering techniques to a benchmark problem (Agarwal, Morris & Mani 2004) of a two-dimensional parallel jet (Mach number = 0.756) that is excited by a time-harmonic spatially compact Gaussian source located at the origin. In this section, we use a Cartesian coordinate system (x, y), where x and y represent streamwise and cross-stream directions, respectively. The results presented in the present section are normalised by the half-velocity radial distance r_0, centreline jet speed U_j and density ρ_j as the length, velocity and density scales, respectively. The (normalised) frequency of excitation $\omega_s = 0.27$ is such that it generates both an acoustic wave and a strong instability wave (figure 1*a*). The solution is obtained by solving the linearised Euler equations (LEE) using an explicit finite-difference scheme. Because the problem is linear and the hydrodynamic wave in this problem is represented by a strong instability wave, it is an ideal problem to test the filtering techniques of their ability to separate hydrodynamic and acoustic components from fluid-flow equations.

The pressure component is filtered using two methods. For the differential filter, the d'Alembertian filter from (2.33) is applied at every time step to obtain $\Box^2 p$. For the convolution filter, the pressure is stored over five periods $T_s = 2\pi/\omega_s$ and 125 time frames are used to compute the filtered solution in the frequency domain. Instead of filtering out the acoustic waves directly, the sum of two Gaussian windows is used, one centred at k_0 and the other at $-k_0$, i.e.

$$W(\boldsymbol{k}, \omega) = \exp\left[-\frac{(k_x - k_0)^2}{2\sigma^2}\right] + \exp\left[-\frac{(k_x + k_0)^2}{2\sigma^2}\right], \tag{3.1}$$

where k_x is the streamwise wavenumber, $k_0 = 0.88$ and $\sigma = 0.13$. The corresponding filtered pressure is denoted $\mathscr{G}p$. The filter is defined after examining the pressure field in the wavenumber domain. For $\omega = \pm\omega_s$, the instability waves dominate the wavenumber spectrum in a very narrow band centred around $\pm k_0$. The value of k_0 also matches that obtained by finding the eigenvalue for the instability wave (Agarwal *et al.* 2004). We expect the filter of (3.1) to capture the instability wave without distorting it.

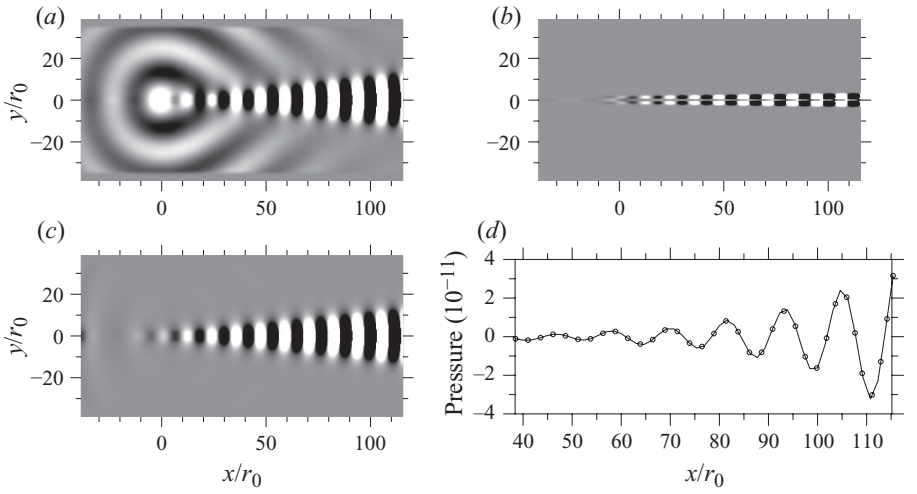

FIGURE 1. Comparison of total pressure, p, with the filtered pressure obtained by applying the differential and convolution filters. The uniform mean static pressure, p_0, has been subtracted in each plot. The linear contour scale in (*a*)–(*c*) ranges from -2.5×10^{-11}Pa (black) to 2.5×10^{-11}Pa (white). (a) Total pressure p, (b) filtered pressure $\bar{p} = l^2 \times \Box^2 p$, (c) filtered pressure $\bar{p} = \mathscr{G}p$ and (d) profiles of hydrodynamic pressure (solid line) and filtered pressure $\mathscr{G}p$ (circles), along $y = 11.5r_0$.

Note that it is possible to use a filter that discards the waves satisfying (2.37) rather than one centred on hydrodynamics as in (3.1). However, care must be taken in the present problem because of the strong hydrodynamic field and its proximity, in the wavenumber domain, to the acoustic radiation circle. The data must be windowed prior to taking the Fourier transform, e.g. by using a Hann window, to obtain a good enough resolution of the transform (see e.g. Shin & Hammond 2008). Failing to do so is equivalent to using a rectangular window, whose roll-off is too slow in this case. The high side lobes and slow roll-off of the rectangular window lead to a large amount of spectral leakage, which fully contaminates the radiation circle. Nevertheless, for a diverging base flow, it may not be necessary to window the data. Following such a procedure, we obtain a similar result to that shown in figure 1(*c*). However, the filter of (3.1) was found to be easier to implement.

3.2. *Results and discussion*

The pressure field $p(x, t)$ is plotted in figure 1(*a*). The figure shows the presence of two kinds of waves radiating from the origin: acoustic waves radiating to the far field and hydrodynamic waves growing in the downstream direction along the x-axis. Figures 1(*b*) and 1(*c*) show the filtered pressure obtained using, respectively, the d'Alembertian filter $\Box^2$ and the Gaussian filter $\mathscr{G}$. In order to compare $\mathscr{G}p$ with p, which does not have the same physical dimension, the former has been multiplied by a factor $l^2 = 2.5$, computed so as to have $l^2 \cdot \max(\mathscr{G}p) = \max(p)$. A comparison between an exact analytical solution for the hydrodynamic pressure obtained by Agarwal *et al.* (2004) and $\mathscr{G}p$ along the line $y = 11.5r_0$ is presented in figure 1(*d*). The uniform mean static pressure p_0 has been subtracted from these figures.

Figures 1(*b*) and 1(*c*) clearly show that both d'Alembertian and Gaussian filters render the pressure field non-radiating. However, the d'Alembertian filter changes the structure of the hydrodynamic waves. This is a direct consequence of the fact that (2.38) is not satisfied by the d'Alembertian operator. On the contrary, the base

flow obtained using the Gaussian filter is in very good agreement with the original flow, in the region where the instability wave is dominant. This can be seen qualitatively by comparing figures 1(*a*) and 1(*c*) and quantitatively in figure 1(*d*).

Thus, convolution filters are flexible enough to design optimal non-radiating filters in the frequency domain, even though the acoustic fluctuations have a much smaller amplitude than the hydrodynamic ones.

4. Sources of sound in an axisymmetric jet flow

4.1. *Problem description*

We now consider a nonlinear problem in which an axisymmetric jet is excited by two discrete-frequency axisymmetric disturbances at the jet exit. The frequencies are chosen to trigger some instability waves in the flow. These instability waves grow downstream and interact nonlinearly, generating acoustic waves. The Mach number of the jet is 0.9 and the Reynolds number is 3600. The base mean flow is chosen to match the experimental data of Stromberg, McLaughlin & Troutt (1980).

Suponitsky & Sandham (2009) performed direct numerical simulations of the compressible Navier–Stokes equations for this problem. In their simulations the mean flow was prescribed by imposing time-independent forcing terms. They ran simulations with different combinations of excitation frequencies and amplitudes. The data used here correspond to the combination with the largest acoustic radiation. The two excitation frequencies are $\omega_1 = 2.2$ and $\omega_2 = 3.4$. Sound radiates mainly at the difference frequency $\Delta\omega = 1.2$. The results presented in this section have been normalised by using the jet diameter D, jet exit speed U_j and the ambient density as the length, velocity and density scales, respectively. Note that despite the high Mach number, the theory of § 2 can be applied because the numerical procedure prevents the flow from becoming fully turbulent.

4.2. *Flow decomposition*

In order to apply the convolution filtering technique for flow decomposition, we first need to obtain the FT of the flow field. In general this involves transforming in four (time and three space) dimensions. However, given the axisymmetric nature of the present problem, the spatial transforms can be carried out in two dimensions: by applying a Hankel transform (HT) in the radial direction and a Fourier transform in the axial direction. The Hankel transform is carried out numerically using the quasi-discrete Hankel transform of Guizar-Sicairos & Gutiérrez-Vega (2004).

For a given flow variable q, the algorithm for obtaining the non-radiating variable $\overline{q}$ is as follows:

(*a*) interpolate and zero pad the data (to avoid aliasing) in the physical space,
(*b*) compute and remove the time-averaged variable q_0,
(*c*) compute the FT in the axial direction and the HT in the radial direction,
(*d*) multiply by the filter window W,
(*e*) compute the inverse Hankel transform and the inverse Fourier transform,
(*f*) unpad the data and add back q_0.

Mathematically, the filtering procedure can be written as

$$\overline{q} = q_0 + \mathrm{HT}^{-1} \circ \mathrm{FT}^{-1}(\mathrm{HT} \circ \mathrm{FT}(q - q_0) \times W). \tag{4.1}$$

In the above equation, if q is the radial component of a vector, such as ρv_r or f_r, then HT denotes the Hankel transform of order 1. Otherwise, HT denotes the Hankel transform of order 0.

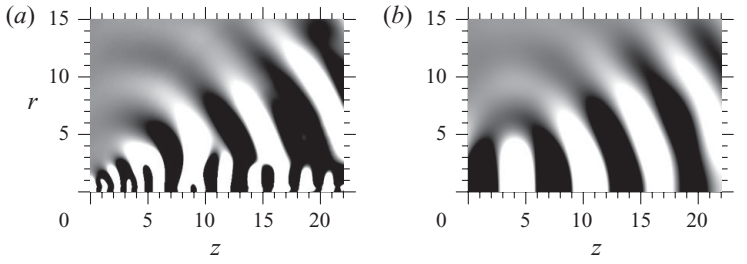

FIGURE 2. Pressure fields for a single time frame. In (*a*), low frequency components p_0 have been removed for plotting. The linear contour scale ranges from -5×10^{-6} (black) to 5×10^{-6} (white). (a) Total pressure p and (b) radiating pressure $p'=p-\bar{p}$.

The window W should satisfy conditions (2.37) and (2.38). For a given frequency ω, we want W to have a value of zero in a narrow band around $|\boldsymbol{k}|=|\omega|/c_\infty=k_{co}$ and one everywhere else. We use a narrow Butterworth band-reject filter to achieve this:

$$W(\boldsymbol{k})=\left(1+\frac{|\boldsymbol{k}|\sigma}{|\boldsymbol{k}|^2-k_{co}^2}\right)^{-4}, \tag{4.2}$$

where σ controls the width of the stop band and k_{co} is the cutoff frequency. In the present problem, the noise radiates mainly at the difference frequency, $\Delta w=\omega_2-\omega_1$. For this frequency, $k_{co}=1.2$. We choose a value of 0.25 for σ.

Note that the algorithm described above assumes that sound is radiating only at the frequency $\Delta\omega$. This is a good approximation for the flow field we are studying here. In the general case, in which sound is radiating at a broad range of frequencies, the algorithm described above can be applied frequency by frequency to the temporal Fourier transform of the flow field.

4.2.1. *Results and discussion*

The success of the filtering operation is verified by examining the radiating part of the pressure field ($p'=p-\bar{p}$), which should contain no hydrodynamic components. Figures 2(*a*) and 2(*b*), respectively, show total pressure p (excluding time-averaged p_0) and radiating pressure p'. They demonstrate that a clear identification of the radiating components has been achieved since p' contains no hydrodynamic component. This shows that using this filtering procedure we are able to obtain the filtered field to a very high order of accuracy because we are subtracting two large quantities (p and $\overline{p}$) to obtain a much smaller quantity (p'). More precisely, we find that p' is three orders of magnitude smaller than $\overline{p}$ along the jet centreline and $\overline{p}-p_0$ is two orders of magnitude smaller than p_0. Similar results have been obtained using the same filter for the other flow variables. This validates the hypothesis that the acoustic field is much smaller than the hydrodynamic field, which in turn is much smaller than the corresponding time-averaged components.

The above filtering procedure is equivalent to convolving the flow with a mask. In the vicinity of the boundary, a part of the mask will lie outside the computational domain, where the flow is set to zero due to zero padding. This leads to inaccuracies near boundaries. To restrict this effect to small regions, the filter must be narrow in the space–time domain. Unfortunately, optimal non-radiating filters must also be narrow in the wavenumber–frequency domain, which is impossible. A trade-off must be made between these two requirements. As can be seen in figure 2, p' is over-estimated in the

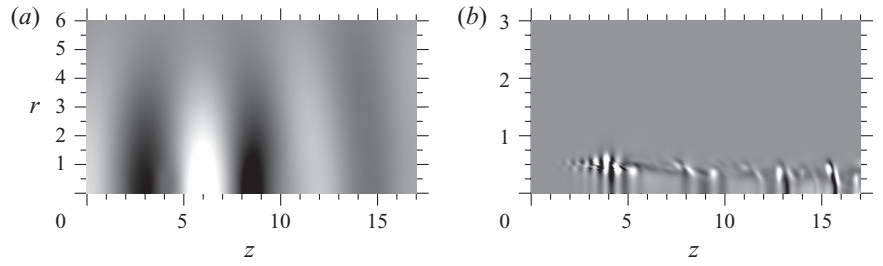

FIGURE 3. Sound sources for a single time frame. The contour scale ranges from -2×10^{-5} (black) to 2×10^{-5} (white) in (a) and -5×10^{-2} (black) to 5×10^{-2} (white) in (b). (a) Sound source s_1 associated with a non-radiating base flow and (b) sound source s_2 associated with a time-averaged base flow.

first four jet diameters. One possible solution would be to extend the computational domain upstream in the simulations.

4.3. *Sound sources*

We compute the physical noise source s_1 from (2.29). To compare s_1 with noise sources obtained by means of classical acoustic analogies (based on time-averaged base flows), we also compute the noise source s_2 associated with a time-averaged base flow. The noise source s_2 is defined as (see the Appendix)

$$s_2 \equiv -\frac{\partial^2}{\partial x_i \partial x_j}\left(\frac{1}{\rho_0}(\rho v_i)''(\rho v_j)'' - \frac{\widehat{v_j}}{\rho_0}(\rho v_i)''\rho'' - \frac{\widehat{v_i}}{\rho_0}(\rho v_j)''\rho'' + \frac{\widehat{v_i}\widehat{v_j}}{\rho_0}\rho''^2\right)'' - \frac{1}{2}\gamma(\gamma-1)\frac{\partial^2}{\partial x_i \partial x_i}\left(\pi_0^{\gamma-2}(\pi)''^2\right)'', \quad (4.3)$$

where subscript '0' and double primes denote, respectively, the time-averaged and unsteady parts of the flow field. The hat accents represent Favre averaging for the steady base flow, i.e. $\widehat{v_i} = (\rho v_i)_0/\rho_0$.

We have validated the sources by solving the LEE driven by these sources. For s_2, the base flow is steady and the pressure solution contains both hydrodynamic and acoustic components. For s_1, the base flow is unsteady but for simplicity we approximate it to be steady (see § 2.1). We find that the pressure field of the LEE solution only contains radiating components and is quantitatively in good agreement with the radiating field obtained directly from DNS (see Sinayoko & Agarwal 2010*b* for details).

Figure 3(a) shows an instantaneous contour plot of s_1 in the physical domain for $0\leqslant r\leqslant 6.0$ and $0\leqslant z\leqslant 17$. Figure 3(b) shows a similar contour plot for s_2 for $0\leqslant r\leqslant 3.0$ and $0\leqslant z\leqslant 17$. The source distribution is different in the two cases. With the non-radiating base flow, the source s_1 is spread over the first four jet diameters in the radial direction, and peaks around $z=6$ in the axial direction, which corresponds to the end of the potential core. The source decays for $z\geqslant 10$. With the time-averaged base flow, the source s_2 is distributed within the jet ($r<0.5$) and along the shear layer ($r=0.5$) and appears to be maximal around $z=4$. The source s_1 exhibits mostly some relatively large structures of the order of the acoustic wavelength $2\pi c_\infty/\Delta\omega = 5.8$, while s_2 involves smaller structures. In terms of amplitude, the peak value of s_2 is three orders of magnitude greater than that of s_1. This can be explained as follows: since s_1 is purely radiating (from (2.24)), it does not contain any hydrodynamic component, which is not the case for s_2. These hydrodynamic components are also

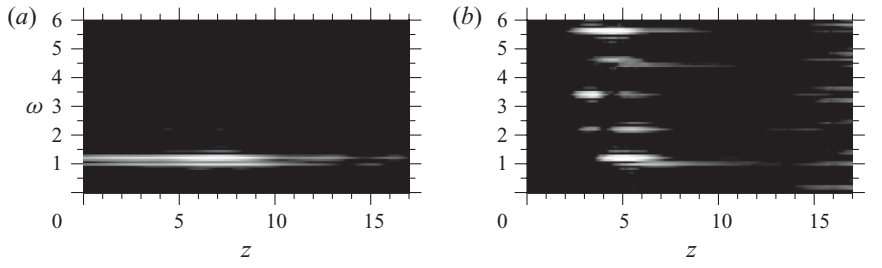

FIGURE 4. Power spectral density for (*a*) source s_1 (non-radiating base flow) along $r=0$, (*b*) source s_2 (time-averaged base flow) along $r=0.25$. The contour scale ranges from -85 dB (black) to -70 dB (white) in (*a*) and -25 dB (black) to -10 dB (white) in (*b*).

three orders of magnitude greater than the acoustic components, as explained in § 4.2. The source s_2 drives both hydrodynamics and acoustics, whereas s_1 only generates sound.

Further physical insight can be obtained by looking at the power spectral density (PSD) of these sources. Figure 4(*a*) shows the PSD of source s_1 for $r=0$, where s_1 is maximum. Figure 4(*b*) shows the PSD of s_2 for $r=0.5$, where s_2 is dominant. These figures indicate that s_1 is dominated by the frequency $\Delta\omega=1.2$, whereas s_2 contains several other frequencies, e.g. $\omega_1=2.2$, $\omega_2=3.4$, $2\omega_1=4.4$ and $\omega_1+\omega_2=5.6$. We expect the true source of sound to have the frequency of acoustic waves, i.e. $\Delta\omega$. In that respect, the source s_1 based on a non-radiating base flow is more physical than s_2 which is based on a time-averaged base flow. Only a small portion of s_2 generates sound.

5. Conclusions

It is possible to decompose flow field variables satisfying the unbounded Navier–Stokes equations into acoustically radiating and non-radiating components by means of linear convolution filters. Following such a decomposition it is possible to obtain a well-defined source for aerodynamically generated noise. Unlike source terms based on classical acoustic-analogy approaches, the resulting source terms are a function of only the non-radiating components and they produce only acoustic waves.

The flow filtering technique presented in this paper is a post-processing technique applicable once the solution of the compressible Navier–Stokes equations has been obtained. The method can be readily applied to a CFD flow simulation even if the acoustic field is not adequately resolved, as the noise sources are a function of only the non-radiating components.

We are indebted to Dr V. Suponitsky and Professor N. Sandham, who carried out the direct numerical simulation for the second test case used in this paper. We would like to thank Professor P. White and Drs G. Gabard, P. Jordan and R. Sandberg for many useful discussions. This project is funded by the Engineering and Physical Sciences Research Council under grant EP/F003226/1. The authors also gratefully acknowledge Rolls-Royce plc for their financial support.

Appendix. Sources of sound for a time-averaged base flow

For a flow decomposition method based on a time-averaged base flow, any flow variable q is decomposed as

$$q = q_0 + q'', \tag{A 1}$$

where q_0 and q'' denote, respectively, the steady (time-averaged) and unsteady part of q.

Since taking the time average is a linear operation, following the procedure of § 2.2 leads to

$$\frac{\partial \rho''}{\partial t} + \frac{\partial}{\partial x_j}(\rho v_j)'' = 0, \tag{A 2}$$

$$\frac{\partial}{\partial t}(\rho v_i)'' + \frac{\partial}{\partial x_j}(\rho v_i v_j)'' + \frac{\partial (\pi^\gamma)''}{\partial x_i} = 0, \tag{A 3}$$

$$\frac{\partial \pi''}{\partial t} + \frac{\partial}{\partial x_j}(\pi v_j)'' = 0. \tag{A 4}$$

The term $\rho v_i v_j$ can be decomposed as

$$\rho v_i v_j = \begin{cases} (a)\ \rho_0 \widehat{v_i}\widehat{v_j} + \\ (b)\ \widehat{v_j}(\rho v_i)'' + \widehat{v_i}(\rho v_j)'' - \widehat{v_i}\widehat{v_j}\rho'' + \\ (c)\ \dfrac{1}{\rho_0}(\rho v_i)''(\rho v_j)'' - \dfrac{\widehat{v_j}}{\rho_0}(\rho v_i)''\rho'' - \dfrac{\widehat{v_i}}{\rho_0}(\rho v_j)''\rho'' + \dfrac{\widehat{v_i}\,\widehat{v_j}}{\rho_0}\rho''^2 + O(\rho''^3), \end{cases} \tag{A 5}$$

where we have introduced the Favre-averaged hat quantities

$$\widehat{v_i} = \frac{(\rho v_i)_0}{\rho_0}, \tag{A 6}$$

which are analogous to $\widetilde{v_i}$ but use a steady base flow rather than a non-radiating base flow. The terms (a–c) of (A5) behave as follows:

(a) is steady, i.e. $(a)'' = 0$,

(b) is purely unsteady, i.e. $(b)'' = (b)$, and corresponds to interaction between the mean flow and the fluctuating flow,

(c) is nonlinear in unsteady variables and contains the sound sources.

The term $(\pi^\gamma)''$ is decomposed as follows:

$$\pi^\gamma = (\pi_0 + \pi'')^\gamma = \pi_0^\gamma + \gamma \pi_0^{\gamma-1}\pi'' + \tfrac{1}{2}\gamma(\gamma-1)\pi_0^{\gamma-2}\pi''^2 + O(\pi''^3), \tag{A 7}$$

$$(\pi^\gamma)'' \approx \gamma \pi_0^{\gamma-1}\pi'' + \tfrac{1}{2}\gamma(\gamma-1)\pi_0^{\gamma-2}(\pi''^2)''. \tag{A 8}$$

Finally, the term πv_j is decomposed as follows:

$$\pi v_j = \begin{cases} (a)\ \dfrac{\pi_0}{\rho_0}(\rho v_j)_0 + \\ (b)\ \dfrac{\pi_0}{\rho_0}(\rho v_j)'' + \widehat{v_j}\pi'' - \dfrac{\pi_0}{\rho_0}\widehat{v_j}\rho'' + \\ (c)\ \dfrac{1}{\rho_0}\pi''(\rho v_j)'' - \dfrac{\widehat{v_j}}{\rho_0}\rho''\pi'' - \dfrac{\pi_0}{\rho_0^2}\rho''(\rho v_j)'' + \dfrac{\pi_0\widehat{v_j}}{\rho_0^2}\rho''^2 + O(\rho''^3), \end{cases} \tag{A 9}$$

where expression (a) of (A9) has no unsteady part, expression (b) of (A9) corresponds to interaction terms and expression (c) of (A9) to source terms. However, expression (c) of (A9) can be expressed as

$$\frac{1}{\rho_0}\left(\pi'' - \frac{\pi_0}{\rho_0}\rho''\right)\left((\rho v_j)'' - \rho''\widehat{v_j}\right). \tag{A 10}$$

Using the hypothesis of homentropy, i.e. $p = \alpha\rho^{\gamma}$, it can be shown that

$$\pi'' = \alpha^{1/\gamma}\rho'', \tag{A 11}$$

where $\alpha = (\pi_0/\rho_0)^{\gamma}$, so (c) of (A9) is equal to zero.

We can now rewrite equations (A 2)–(A 4) by pushing the sound sources to the right-hand side and leaving the propagation terms on the left-hand side

$$\frac{\partial \rho''}{\partial t} + \frac{\partial}{\partial x_j}(\rho v_j)'' = 0, \tag{A 12}$$

$$\frac{\partial}{\partial t}(\rho v_i)'' + \frac{\partial}{\partial x_j}(\widehat{v_j}(\rho v_i)'' + \widehat{v_i}(\rho v_j)'' - \widehat{v_i}\widehat{v_j}\rho'') + \gamma\frac{\partial}{\partial x_i}\pi_0^{\gamma-1}\pi'' = f_{2i}, \tag{A 13}$$

$$\frac{\partial \pi''}{\partial t} + \frac{\partial}{\partial x_j}\left(\frac{\pi_0}{\rho_0}(\rho v_j)'' + \widehat{v_j}\pi'' - \frac{\pi_0}{\rho_0}\widehat{v_j}\rho''\right) = 0, \tag{A 14}$$

where the momentum equation source term f_{2i} is defined as

$$f_{2i} \equiv -\frac{\partial}{\partial x_j}\left(\frac{1}{\rho_0}(\rho v_i)''(\rho v_j)'' - \frac{\widehat{v_j}}{\rho_0}(\rho v_i)''\rho'' - \frac{\widehat{v_i}}{\rho_0}(\rho v_j)''\rho'' + \frac{\widehat{v_i}\widehat{v_j}}{\rho_0}\rho''^2\right)'' - \frac{1}{2}\gamma(\gamma-1)\frac{\partial}{\partial x_i}\left(\pi_0^{\gamma-2}(\pi)''^2\right)''. \tag{A 15}$$

The wave-equation noise source analogous to (2.29) is given by

$$s_2 = \frac{\partial f_{2i}}{\partial x_i}. \tag{A 16}$$

REFERENCES

Agarwal, A., Morris, P. J. & Mani, R. 2004 Calculation of sound propagation in nonuniform flows: suppression of instability waves. *AIAA J.* **42** (1), 80–88.

Cabana, M., Fortuné, V. & Jordan, P. 2008 Identifying the radiating core of Lighthill's source term. *Theor. Comput. Fluid Dyn.* **22** (2), 87–106.

Crighton, D. G. 1975 Basic principles of aerodynamic noise generation. *Prog. Aerosp. Sci.* **16**, 31–96.

Dowling, A. P. & Ffowcs Williams, J. E. 1983 *Sound and Sources of Sound*. Ellis Horwood.

Freund, J. B. 2001 Noise sources in a low-Reynolds-number turbulent jet at Mach 0.9. *J. Fluid Mech.* **438**, 277–305.

Goldstein, M. E. 1976 *Aeroacoustics*. McGraw-Hill International.

Goldstein, M. E. 2003 A generalized acoustic analogy. *J. Fluid Mech.* **488**, 315–33.

Goldstein, M. E. 2005 On identifying the true sources of aerodynamic sound. *J. Fluid Mech.* **526**, 337–347.

Goldstein, M. E. 2009 A theoretical basis for identifying the sound sources in a turbulent flow. *Intl J. Aeroacoust.* **8** (4), 283–300.

Guizar-Sicairos, M. & Gutiérrez-Vega, J. C. 2004 Computation of quasi-discrete Hankel transforms of integer order for propagating optical wave fields. *J. Opt. Soc. Am.* A **21** (1), 53–58.

Lilley, G. M. 1974 On the noise from jets. In *AGARD Conference Proceedings No. 131 on Noise Mechanisms*, *Brussels, Belgium*, pp. 13–21.

Shin, K. & Hammond, J. 2008 *Fundamentals of Signal Processing for Sound and Vibration Engineers*. Wiley.

Sinayoko, S. & Agarwal, A. 2010*a* Flow filtering and the physical sources of aerodynamic sound. In *IUTAM Symposium on Computational Aeroacoustics for Aircraft Noise Prediction*, Southampton, UK.

Sinayoko, S. & Agarwal, A. 2010*b* On computing the physical sources of jet noise. *AIAA Paper* 2010-3962. 16th AIAA/CEAS Aeroacoustics Conference, Stockholm, Sweden.

Stromberg, J. L., McLaughlin, D. K. & Troutt, T. R. 1980 Flow field and acoustic properties of a Mach number 0.9 jet at a low Reynolds number. *J. Sound Vib.* **72** (2), 159–176.

Suponitsky, V. & Sandham, N. D. 2009 Nonlinear mechanisms of sound radiation in a subsonic flow. *AIAA Paper* 2009-3317. 15th AIAA/CEAS Aeroacoustics Conference, Miami, Florida, USA.

Tinney, C. E. & Jordan, P. 2008 The near pressure field of co-axial subsonic jets. *J. Fluid Mech.* **611**, 175–204.